[15]Cole, D., Glauser, M., and Guezennec, Y., "An Application of the Stochastic Estimation to the Jet Mixing Layer," *Physics of Fluids*, Vol. 4, No. 1, 1991, pp. 192–194.

[16]Picard, C., and Delville, J., "Pressure Velocity Coupling in a Subsonic Round Jet," *Engineering Turbulence Modeling and Experiments—4*, edited by W. Rodi and D. Laurence, Elsevier, Amsterdam, 1999, pp. 443–452.

[17]Guezennec, Y., "Stochastic Estimation of Coherent Structures in Turbulent Boundary Layers," *Physics of Fluids A*, Vol. 1, No. 6, 1989, pp. 1054–1060.

[18]Murray, N., and Ukeiley, L. "Estimating the Shear Layer Velocity Field Above an Open Cavity from Surface Pressure Measurements," AIAA Paper 2002-2866, June 2002.

[19]Sinha, N., Hosangadi, A., and Dash, S., "The CRAFT NS Code and Preliminary Applications to Steady/Unsteady Reaction, Multi-Phase Jet/Plume Flowfield Problems," Chemical Propulsion Information Agency, Publ. 568, Columbia, MD, May 1991.

[20]Sinha, N., Arunajatesan, S., and Ukeiley, L., "High Fidelity Simulation of Weapons Bay Aeroacoustics and Active Flow Control," AIAA Paper 2000-1968, June 2000.

W. J. Devenport
Associate Editor

Control of a Plane Jet by Fluidic Wall Pulsing

J. C. Béra[*]
Ecole Centrale de Lyon,
69134 Ecully, France
M. Ben Chiekh[†]
Ecole Nationale d'Ingénieurs de Monastir,
Monastir 5000, Tunisia
and
M. Michard,[‡] G. Comte-Bellot,[§] and M. Sunyach[¶]
Ecole Centrale de Lyon,
69134 Ecully, France

I. Introduction

PULSED injection at a wall constitutes an efficient way to control and manipulate flows. Significant results have been obtained on both external and internal flows. For example, the control of the boundary-layer separation of external flows was investigated by Smith et al.[1] and Béra et al.[2] for cylinders and by Seifert et al.[3] and MacManus and Magill[4] for wings. In both cases control applied at the wall could delay the separation and increase lift. For internal flows Kwong and Dowling[5] and Ben Chiekh et al.[6] showed that such a control can increase the lateral mixing, hence improving the mean pressure recovery in diffusers.

The ability of pulsed injection actuators to control jets was extensively studied by Smith and Glezer,[7,8] who implemented vectoring control of plane freejets. A synthetic jet actuator (i.e., a zero-net-mass-flux injection made of alternate blowing and sucking) was

[*]Assistant Professor, Laboratory of Fluid Mechanics and Acoustics; jean-christophe.bera@ec-lyon.fr.

[†]Graduate Student, Laboratoire d'Etudes des Systèmes Thermiques et Energétiques.

[‡]Research Engineer, Laboratory of Fluid Mechanics and Acoustics.

[§]Professor Emeritus, Laboratory of Fluid Mechanics and Acoustics. Senior Member AIAA.

[¶]Professor, Laboratory of Fluid Mechanics and Acoustics.

placed adjacent to the exit plane of a primary jet. Flow visualizations and velocity field measurements showed that the primary jet was deviated towards the actuator. In the most recent work[8] the optimized use of a little longitudinal extension of one wall of the synthetic jet led to a deviation angle of nearly 30 deg for a jet centerline velocity of 7 m/s (based on this velocity: $Re_{jet} \approx 6 \times 10^3$, $c_{\mu\,control} \approx 0.5$) and 12 deg for a jet centerline velocity of 17 m/s ($Re_{jet} \approx 14 \times 10^3$, $c_{\mu\,control} \approx 0.09$).

Pack and Seifert[9] controlled a circular turbulent jet using a short wide-angle diffuser attached to the exit of the jet. High-amplitude, periodic streamwise excitation at the junction between the jet exit and the diffuser inlet enhanced the mixing and provided a jet deflection towards the diffuser wall. The results showed an obvious effect of the diffuser: at $Re_{jet} \approx 30 \times 10^3$ and for $c_{\mu\,control} \approx 0.05$, a deflection angle of 8 deg was registered in the presence of a 30-deg diffuser, vs 2 deg without diffuser.

Parekh et al.[10] applied the control to mixing enhancement by using two pulsed injections, one on each side of the jet, either longitudinal or normal to the main flow. Working on circular and plane jets, they showed that different modes of jet excitations are possible. The direct numerical simulations of Freund and Moin[11] pointed out the complexity of the control mechanism, notably in showing the role of both the injection angle and the Strouhal number.

The present work is mainly an extension to the works of both Parekh et al.[10] and Pack and Seifert.[9] A two-dimensional jet was considered, and excitation was applied on both sides of the jet. A streamwise excitation was retained as being more efficient than a cross-stream excitation. A short large-angle diffuser was also added at the jet exit as this significantly amplified the pulsing control introduced in the streamwise direction. All measurements were made using particle image velocimetry (PIV), so that global maps could be obtained for the analysis of the physical phenomenon involved. The measured two-dimensional fields were then either mean averaged or phase averaged with a condition on the control phase.

II. Experimental Setup

A. Wind-Tunnel Facility

Experiments were performed on a jet issuing from a rectangular nozzle (height $h = 3$ cm, span $4h$). The flow was generated by a low-turbulence subsonic wind tunnel ended by a plane contraction of ratio four and a rectangular channel (length $9h$). The mean velocity at the jet exit was $U_0 = 18$ m/s, and the jet Reynolds number was 36×10^3. The jet exit was connected to a symmetrical two-dimensional divergent (angle 2×45 deg, area ratio 4, and therefore outlet height 12 cm). The divergent was opened on a plenum. Perspex walls were used to provide optical access.

B. Wall Pulsed Control

A pair of pulsed injection actuators was positioned at the jet exit, one actuator symmetrically on each wall of the two-dimensional model. For each actuator the injector was a slit, placed just at the beginning of the diffuser wall, just at the corner: Fig. 1 shows details
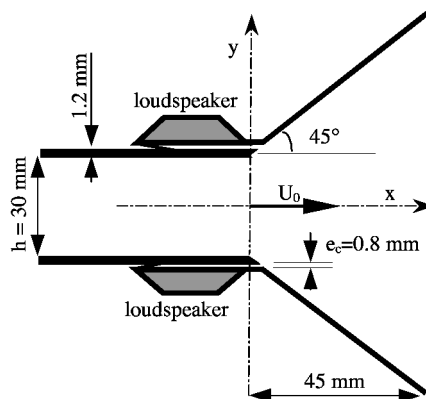

Fig. 1 Schematic of the experiment and axis definitions.

of the setup. The actuator was designed to generate a streamwise excitation, which can manipulate the shear layer without destroying it.

The actuators were similar to the electrodynamical "synthetic jet" generators described in detail by Béra et al.[12] The actuator slit dimensions were $e_c = 0.8$ mm in width and 95 mm in span. Each slit was fed by a pulsed cavity having as cover the wall upstream of the diffuser. Pressure fluctuations in the cavity were generated by a loudspeaker fed by a sinusoidal electric current. In the absence of the jet, the flow created by the actuators was measured using hot-wire anemometry. The velocity signal at the slit exit was sinusoidal: amplitude $U_c = 32$ m/s and frequency $f_c = 100$ Hz. The frequency chosen gave a Strouhal number of $Sr = f_c h / U_c = 0.17$, corresponding approximately to the half of the most amplified frequency of the unforced jet. It is close to $Sr = 0.20$, the value found by the numerical predictions of Freund and Moin[11] for the most efficient spreading of a the jet. The chosen rms actuator velocity was close to that of the jet velocity, following previous experiments in our laboratory. This velocity corresponds to a momentum coefficient by unit span, near the central plane and for dual control, of

$$c_\mu = 2 \frac{e_c \langle u^2_{\text{contrôle}} \rangle}{h U_0^2} = 2 \frac{e_c U_c^2 / 2}{h U_0^2} \approx 2 \times 0.04$$

Four configurations of control were tested: 1) upper-side control with one actuator on, 2) lower-side control with one actuator on, 3) dual control with upper and lower actuators working in phase, and 4) dual control with upper and lower actuators working exactly out of phase (180 deg).

C. Velocity Measurement

Instantaneous velocity fields were measured using PIV. The flow was seeded with small oil droplets of approximately 1 to 2 μm in diameter, produced by a smog generator located at the inlet of the wind-tunnel fan. Measurements were carried out with a Dantec system using two coupled YAG laser sources (220-mJ Quantel lasers). Each laser emitted a pulse with a time delay of 50 μs between them. This cycle was repeated at a frequency of about 9 Hz. The light scattered by the seeding particles was recorded with a 1280×1024-pixel Hisense Dantec charge-coupled device (CCD) camera (pixel length 3.4 μm; pitch pixel 6.7 μm). The optical characteristics were magnification ratio = 1/17.6 and focal length/aperture diameter ratio = 2.8. Pairs of raw images were cross correlated by using 32×32-pixel interrogation windows, with a 50% overlap ratio between adjacent windows. The resulting spatial resolution of the PIV measurement was 1.7×1.7 mm. The measurement uncertainty was of the order of 0.2 pixels (Ref. 13), corresponding to 0.5 m/s on the instantaneous velocity measurements. Every field reported in the present investigation was deduced from an average of 200 instantaneous fields, improving notably the measurement accuracy.

D. Postprocessing of PIV Data

The data were processed in two steps. The first step used conventional tools to give us the mean flowfields. The second step involved analytical tools specially developed to accurately obtain the jet-angle deflection, the streamline distribution, and the eddy centers. These calculations were based on work done by Pack and Seifert[9] and Michard et al.[14]

III. Measurements and Interpretation

A. Mean Flow Maps and Profiles

To compare the general aspect of the mean flows, streamlines are plotted in Fig. 2. They clearly show the significant effect of the control on the flow: the jet deviates toward the controlled side in the case of one-side control, and the jet enlarges in every case of control. Moreover, great differences in flow entrainment can be observed between the controlled and uncontrolled jets. Without control the entrainment is low up to $x = 2h$, that is, in the vicinity of the jet restriction, and downstream the surrounding fluid regularly and
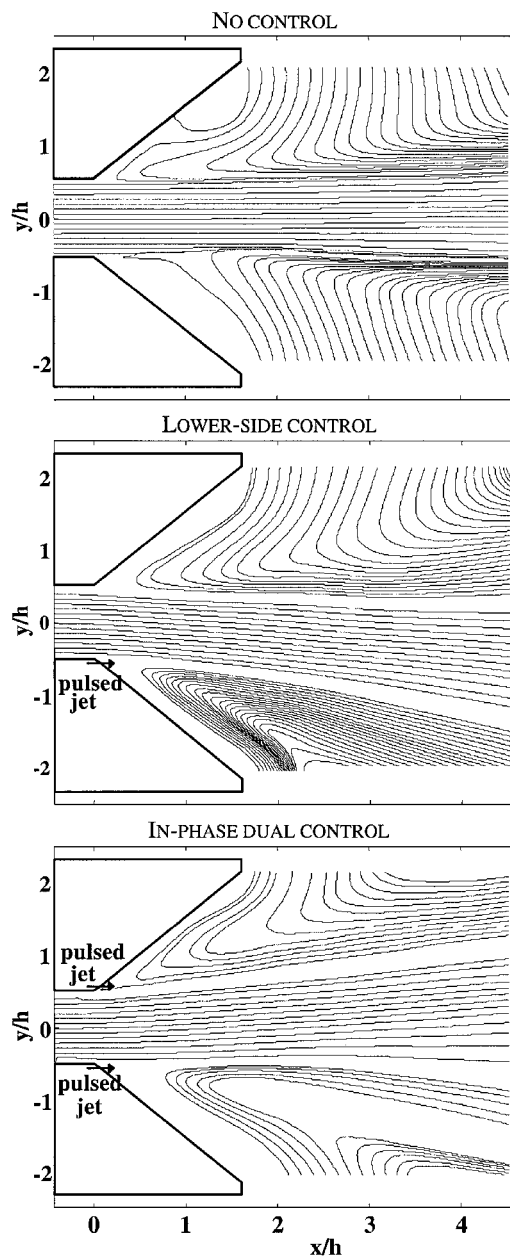

Fig. 2   Streamlines, for different configurations of control (starts of the lines imposed).

symmetrically feeds the jet expansion. Associated with this classic jet behavior, a bubble of zero-mean-velocity fluid is generated on each diffuser wall, around $x = h$ and $y = 1.5h$. With one-side control the bubble is still visible on the uncontrolled side, although its size is reduced. On the controlled side, the bubble completely disappears: an entrainment flux creeps upstream along the diffuser wall to feed the jet expansion inside the diffuser. With both-side control, such an entrainment flux is present on each side of the jet. However, the entrainment caused by the control on each diffuser side seems to be less intense than that generated by the one-side control on the controlled side. Indeed, under one-side control the jet centerline deviates towards the controlled side, which means that jet flow directly feeds the jet enlarging on this side; as a consequence, the reverse flow is more confined near the diffuser wall.

For quantitative study, velocity profiles can be extracted from the PIV velocity fields (Fig. 3). The resulting curves are very smooth, confirming the good quality of the measurements. These profiles reflect the deviation and enlargement of the controlled jets. The most enlarged profiles are obtained when both upper and lower actuators are operating. The two types of dual control provide profiles very similar to each other.
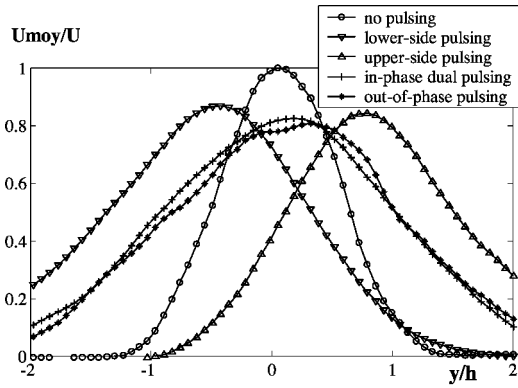
Fig. 3 Mean velocity profiles at $x = 4h$ for the different configurations of control.
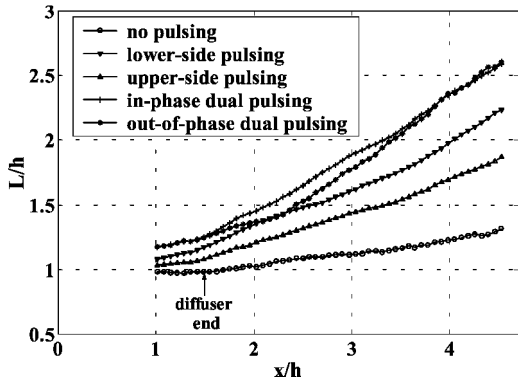

Fig. 4 Jet expansion for the different configurations of control: jet width L, measured at the half of the maximal velocity, as a function of the distance from the jet mouth.

The jet deviation and the jet width are directly calculated from the mean velocity U fields. With the dual pulsing, the flow remains roughly centered despite slightly different velocity distributions between its two sides. It deviates only by 1 deg downward in term of momentum center and between 1 and 3 deg upward in terms of maximal velocity. With the one-side controls, the jet deviations are considerable: the deviation angle is 8 deg downward for lower-side control and 10 deg upward for upper-side control.

The jet widths are represented in Fig. 4. Without control the jet approximately keeps a constant width up to $x = 2h$ from the jet exit, and downstream it expands linearly with a slope of 0.10, in compliance with the previous studies on turbulent plane jets by Kotsovinos.[15] When the control is applied, the flow enlarges as soon as it crosses the jet exit and all along the diffuser. This enlargement is greater for dual control than for one-side control. Downstream from $x = 2h$, the excited jet expands approximately linearly with a slope in the range 0.25–0.35 for one-side pulsing and reaching 0.50 for both-side pulsing either in phase or out of phase.

B. Flow Structures in the Controlled Jets

The large-scale flow structures generated by wall pulsing can be precisely located on each phase-average velocity field. As an illustration, Fig. 5 presents the flowfield for every type of control, at a given pulsing phase at the lower-side actuator. A phase at the end of blowing was selected because the building of the vortex structure is achieved, as described by Béra et al.[12] In each map the eddy centers are detected by eddy-center criterion. Some centers are in the inner part of the diffuser, still close to the actuators. The corresponding phase-average eddy structures are very intense and also clearly visible on the velocity arrows. The other centers observed outside the diffuser correspond to structures generated earlier, convected downstream, and becoming more diffuse. By comparing the phase-averaged maps at different phases of the pulsing (not reported
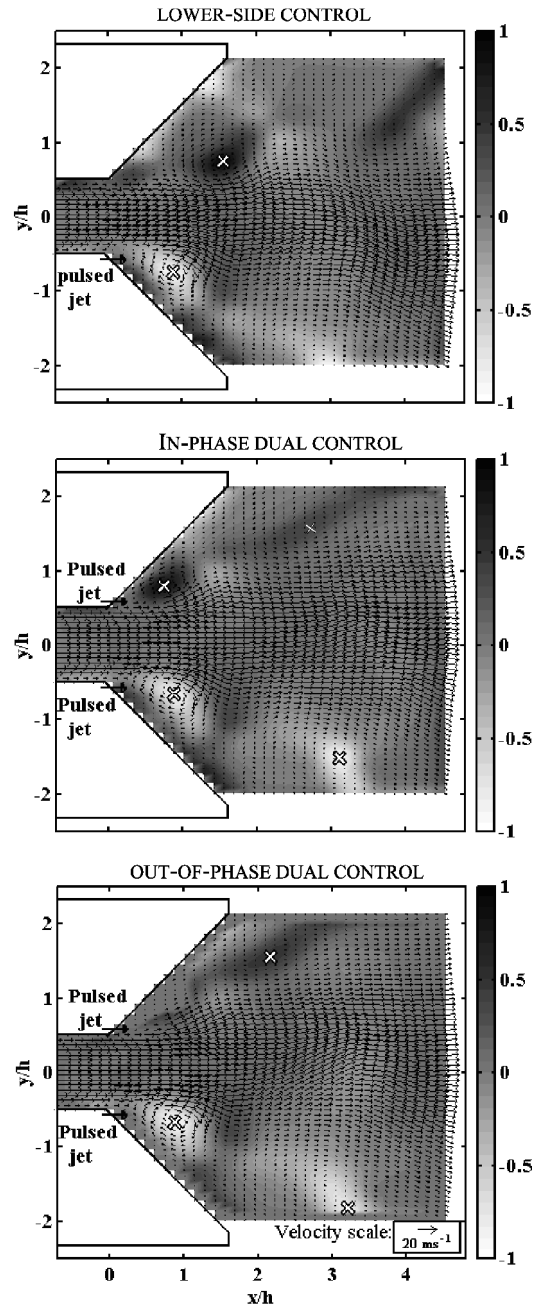

Fig. 5 Phase-average velocity fields ($\rightarrow$) and corresponding maps of phase-average eddy-center criterion (gray level and crosses) at the end of the blowing phase of the lower actuator.

in the present paper), the averaged eddies generated by the control can be followed over the pulsation cycle, showing their progressive convection. Thus, in every case of control the convection velocity can be estimated at $0.42U_0$, which is in the usual range of values for eddy convection velocity in a separated layer.

The eddy-center criterion maps also permit us to point out some differences between the controls. Whereas a large eddy on the lower-side diffuser wall is present at approximately the same place whatever the control, the location of the contrarotating eddy on the other side clearly depends on the type of control. With in-phase pulsing the eddy pattern is approximately symmetrical, in accordance with the in-phase eddy generation and convection. With out-of-phase pulsing the location of the eddies alternate between the top and bottom of the jet, as they progress by convection in the direction of the jet. For the one-side control a contrarotating structure appears on the uncontrolled side. This structure is roughly symmetric to the active structure created by the control, with respect to the axis of

the deviated jet. Physically, it is linked to the unsteady entrainment on the uncontrolled side.

C. Discussion on the Control Mechanism

The phase-averaged measurements bring some physical insight into the control mechanism. Control pulsing affects the flow near the diffuser wall by means of a periodic train of eddies. On one side of these eddies, their flux is part of the jet flow, and on the other side they roll on the diffuser wall with a slight sliding, which is indicated by the reverse flow along the wall. Thus, the presence of a diffuser at the jet mouth would permit the use of the main flow energy to deviate the jet by the Coanda effect. The Coanda effect acts on the periodic train of vortical structures generated by the control, which are attached to the main flow. These structures permit the jet to come closer to the diffuser wall. The present experiment is almost a limiting case where one and only one control structure is always inside the diffuser: the ratio of the control wavelength to the diffuser wall length is about one.

The importance of the suction phase in the control process can also be discussed. As in Smith and Gleser's work,[8] the synthetic jet injector used in the present investigation was not symmetrical, with a slight streamwise extension on one side, so that the suction of the main jet fluid is favored. This direct suction of the jet flow, which appeared to be very efficient in deviating laminar jets,[8] would also have some effect on the turbulent jet being studied. The diffuser wall would then take advantage of this early deviation for the subsequent eddy dynamics.

IV. Conclusions

This experimental investigation has shown the efficiency of a wall pulsing control applied on a plane turbulent jet with a short wide-angle diffuser attached to the jet exit. The wall pulsing increases the jet lateral expansion. Pulsing on both sides of the jet was also found to be the most efficient for lateral expansion: spreading parameter of the order of 2×0.25 have been obtained compared to 0.30 for one-side control and 2×0.10 without control. The inner structure of the jet was found to be strongly modified, with a shortening of the potential core and with the generation of highly periodic large-scale structures. The mechanism of the control was also investigated. The control system generated vortex structures, which stuck to the diffuser wall by the Coanda effect and then enlarged the jet. Concerning the control frequency, it is also interesting to note that it was relatively low, hence permitting extensions towards higher Reynolds numbers and specially higher jet velocities.

References

[1]Smith, D., Amitay, M., Kibens, V., Parekh, D., and Glezer, A., "Modification of Lifting Body Aerodynamics Using Synthetic Jet Actuators," AIAA Paper 98-0209, Jan. 1998.

[2]Béra, J. C., Michard, M., Sunyach, M., and Comte-Bellot, G., "Changing Lift and Drag by Jet Oscillation: Experiments on a Circular Cylinder with Turbulent Separation," European Journal of Mechanics B—Fluids, Vol. 19, 2000, pp. 575–595.

[3]Seifert, A., Bachar, T., Koss, D., Shepsheplovich, M., and Wygnanski, I., "Oscillatory Blowing: Tool to Delay Boundary-Layer Separation," AIAA Journal, Vol. 31, No. 11, 1993, pp. 2052–2060.

[4]MacManus, K., and Magill, J., "Airfoil Performance Enhancement Using Pulsed Jet Separation Control," AIAA Paper 97-1971, July 1997.

[5]Kwong, A. H. M., and Dowling, A. P., "Active Boundary-Layer Control in Diffuser," AIAA Journal, Vol. 32, 1994, pp. 2409–2414.

[6]Ben Chiekh, M., Béra, J. C., Michard, M., and Sunyach, M., "Contrôle par Jet Pulsé de l'Écoulement Dans un Divergent Court à Grand Angle (Pulsed Jet Control of a Short Diffuser)," Compte Rendu de l'Académie des Sciences de Paris, Vol. 328, Série II.b, pp. 749–756.

[7]Smith, B. L., and Glezer, A., "Vectoring and Small-Scale Motions Effected in Free Shear Flows Using Synthetic Jet Acuators," AIAA Paper 97-0213, Jan. 1997.

[8]Smith, B. L., and Glezer, A., "Jet Vectoring Using Synthetic Jets," Journal of Fluid Mechanics, Vol. 458, 2002, pp. 1–34.

[9]Pack, L. G., and Seifert, A., "Periodic Excitation for Jet Vectoring and Enhanced Spreading," AIAA Paper 99-0672, Jan. 1999.

[10]Parekh, D. E., Kibens, V., Glezer, A., Wiltse, J. M., and Smith, D. M., "Innovative Jet Control: Mixing Enhancement Experiments," AIAA Paper 96-0308, Jan. 1996.

[11]Freund, J. B., and Moin, P., "Jet Mixing Enhancement by High-Amplitude Fluidic Actuation," AIAA Journal, Vol. 38, No. 10, 2000, pp. 1863–1870.

[12]Béra, J. C., Michard, M., Grosjean, N., and Comte-Bellot, G., "Flow Analysis of 2D Pulsed Jets by Particle Image Velocimetry," Experiments in Fluid, Vol. 30, No. 5, 2001, pp. 519–532.

[13]Raffel, M., Willert, C. E., and Kompenhans, J., Particle Image Velocimetry—A Practical Guide, Springer-Verlag, Berlin, 1998, pp. 134–146.

[14]Michard, M., Graftieaux, L., Lollini, L., and Grosjean, N., "Identification of Vortical Structures by a Non Local Criterion: Application to PIV Measurement and DNS-LES Results of Turbulent Rotating Flows," 11th Symposium on Turbulent Shear Flows, Session 28, Institut National Polytechnique de Grenoble/CNRS/Université Joseph Fourier, Sept. 1997, pp. 25–30.

[15]Kotsovinos, N. E., "A Note on the Spreading Rate and Virtual Origin of a Plane Turbulent Jet," Journal of Fluid Mechanics, Vol. 77, Pt. 2, 1976, pp. 305–311.

A. Plotkin
Associate Editor

Local Coordinate Approach in Meshless Local Petrov–Galerkin Method for Beam Problems

I. S. Raju*
NASA Langley Research Center,
Hampton, Virginia 23681-2199
and
D. R. Phillips†
Joint Institute for Advancement of Flight Sciences—George Washington University,
Hampton, Virginia 26381-2199

Introduction

MESHLESS methods are increasingly being viewed as an alternative to the finite element method.[1–5] Recently, a meshless local Petrov–Galerkin (MLPG) method has been presented for C^0 and C^1 problems.[4–6] In these methods, moving least-squares (MLS) interpolants[1] are used for C^0 problems, and generalized MLS interpolants are used for C^1 problems.[5] References 2–6 showed excellent performance of the MLPG method for potential and elasticity problems and a good performance for beam problems.

When all of the chosen parameters in the MLPG method are held constant and the number of nodes in the models is consistently increased, the error norms do not decrease; rather they show increases compared to coarser idealizations. The reasons for this behavior are studied. A local coordinate approach to the MLS interpolation is proposed. The proposed local coordinate approach is implemented and evaluated by applying it to three simple test cases.

Behavior of the MLPG Method with Mesh Refinement

The notation of Ref. 5 is used in this Note for brevity and convenience in presentation. The MLPG equations are

$$K_i^{(\text{node})} d + K_i^{(\text{bdy})} d - f_i^{(\text{node})} - f_i^{(\text{bdy})} = 0 \quad (1)$$